International Journal of Sciences: Basic and Applied Research (IJSBAR)

ISSN 2307-4531
(Print & Online)

http://gssrr.org/index.php?journal=JournalOfBasicAndApplied

Morphometric Measurements of the Mesencephalic Aqueduct in Normal Versus Abnormal Canine Brains: In Vivo MRI Study

Aseel K. Hussein[a]*, Jacques Penderis[b], Martin Sullivan[c]

[a]*Current address: College of Veterinary Medicine, Baghdad University, BOX MAIL 28601, KARKH, AL-Dawwdi Mail Office, Baghdad, Iraq*

[b]*Current address: Vet Extra Neurology, Broadleys Veterinary Hospital, Stirling, UK*

[c]*Current address: School of Veterinary Medicine, College of Medicine, Veterinary Medicine & Life Sciences, University of Glasgow, 464 Bearsden Road, Bearsden, Glasgow G61 1QH, UK*

[a]*Email: fall_of_legend2001@yahoo.com*

[b]*Email: jacques.penderis@vet-neurology.co.uk*

[c]*Email: Martin.Sullivan@glasgow.ac.uk*

Abstract

Several conditions are found to be associated with the cerebral stenosis in young and adult in man. This aqueduct has no record in the veterinary field. The aims of this study are to define the normal shape and area of the aqueduct, establish a new parameter (an angle) in normal canine brains and finding out the effect of abnormalities on these parameters. The shape, area, signal intensity and the angle of the mesencephalic aqueduct of five groups were examined in this study. The results representing that the mesencephalic aqueduct normal shape, its angle and signal intensities are well defined and may be altered in abnormalities.

---

* Corresponding author.
E-mail address: fall_of_legend2001@yahoo.com

The angle is also proportionally affected by the head shape of the dog. It is concluded that the mesencephalic aqueduct is changeable in abnormalities and its angle may be applied for defining the significant changes within the aqueduct.

Keywords: Canine; Brain; MRI; Mesencephalic; aqueduct

1. Introduction

Hydrocephalus in children has been sometimes associated with aqueductal stenosis [1]. The latter has been found with in passive hydrocephalus, dementia and urine incontinence in adulthood [2].

The aqueduct is defined as the canal through which cerebrospinal fluid (CSF) passes from the third to the fourth ventricles [3, 4]. In man, it has been defined as the narrowest pathway of the ventricular system that transfers CSF from the third to the fourth ventricles [5, 6], while it has been defined as having an irregular, somewhat having funnel-like shape that extends from the level of the superior colliculus to the intercollicular sulcus [7].

In the veterinary field, a single term is used for describing this canal “the mesencephalic aqueduct” while it has multiple terms in man; namely: cerebral aqueduct, aqueduct of sylvius, the aqueduct of midbrain [8]) and even earlier called the ventricle of the midbrain by Retzius [9].

The lumen of the neural tube at the embryological stage continues as the ventricular system of the brain and the central canal of the spinal cord after birth [4]. In man, the aqueduct is wide at the vesicle stage narrowing later [10].

The shape and size of the aqueduct of sylvius has been measured grossly from cadavers [10] and a lack of correlation was seen with age in children [11]. Using casts of the ventricular system of the canine brain, the length of the mesencephalic aqueduct has been measured [12].

In the veterinary field, the mesencephalic aqueduct was identified on both sagittal and transverse MRI planes [13, 14] and by computed tomography (CT) [15]. The mesencephalic aqueduct was also identified in the feline brain using MRI [16].

Identification of the signal void generated by CSF flow, pulsation or turbulence was best achieved on the axial (transverse) plane in the mesencephalic aqueduct [17]. Indeed it may have a weak signal or be absent if the aqueduct is physiologically narrow but not obstructed. The signal void was absent mostly with obliteration, distortion or other abnormalities of the aqueduct [17], but was not completely dependable as an indication of obstruction of the cerebral aqueduct [18].

The objectives of the study were to:

a. Describe the shape of the mesencephalic aqueduct on MRI scans of canine brains using T2w midline sagittal and transverse planes

b. Calculate the area on T2w midline sagittal plane MRI
c. Define the tecto-tegmental angle (angulation of the mesencephalic aqueduct)
d. Determine the effect of head conformation, bodyweight and age on the above parameters
e. Evaluate the effect of different lesions on the assessment of aque*duct shape, area and angulation.*

2. Materials & methods

This study was approved by the School of Veterinary Medicine ethics committee and the work was carried out in the Small Animal Hospital using a 1.5Tesla MRI unit (Siemens Magnetom Essenza, Siemens Medical Solutions, Camberley, UK). Dogs were grouped according to the diagnosis, that been made based on clinical and imaging findings, as the following:

Control (Normal): Normal MRI brain. Thirty two dogs presented for a variety of conditions where no abnormalities were found on extensive MRI investigation. Breeds included: Boxer 9, Labrador 5, Bichon Frisé 2, Collie 2, Golden retriever 2, Shih-tzu 2 and one of each of the following breeds [Cocker spaniel, German shepherd, Irish setter, Lhasa apso, Lurcher, Miniature schnauzer, Northern Inuit dog, Shetland sheepdog, Staffordshire bull terrier and Tibetan terrier]. Of the 32 dogs, 10 were females and the rest male. The mean of age was 4.9 (±2.9) years (range 1.1-11.1) while, bodyweight was between 7-42kgs (24.45 ±10.71).

Group-1: 31 dogs with neurological changes which were identified clinically and confirmed by MRI [brain tumour, cerebral herniation and encephalitis]. The following breeds were included in this group [Yorkshire terrier 6, Boxer 3, Boston terrier 2, Chihuahua 2, Cocker Spaniel 2, German shepherd 2, Pug 2, and one each of the following breeds: Beagle, Border terrier, Cross breed, Fox terrier, Labrador, Labra-doodle, Lhasa apso, Lurcher, Maltese terrier, Staffordshire bull terrier, Tibetan terrier and West highland white terrier (WHWT)]. The age range was 0.1-13 years (6.4±3.7). Of the 31, eight were females; and bodyweight ranged between 2.7 and 36kgs (12.93±11.31).

Group-2: Three dogs diagnosed with obstructive congenital hydrocephalus. [Cavalier King Charles spaniel (CKCS)-female, Papillon-male and Cross breed-male] with mean age (1.2 ±0.9 years) and bodyweight (3.25±1.06 kgs).

Group-3: Four dogs diagnosed as having abnormal ventriculomegaly Namely: CKCS, Lhasa Apso, Maltese terrier and Miniature poodle. They weighed between 1.8 and 8kgs (5.68±2.93), with an age range of 0.4-19 (8±8.73). There was one female.

Group-4: Seven dogs diagnosed with quadrigeminal cistern cysts [Chihuahua 4 and one of CKCS, Maltese terrier and Yorkshire terrier breeds]. Their bodyweights were between 1.7-8 (3.66±2.08) and age range was 1.3-10.6 (4.83±3.46). This group had two females and five males.

2.1 Measurements of the mesencephalic aqueduct

A T2w sequence, using a midline sagittal slice and a transverse slice at the level of the colliculi, allowed

generation of images where the shape of the aqueduct was clearly identified (Figure 1). Specific measurements of aqueduct were taken from the mid-sagittal slice. The DICOM images were examined using Clear Canvas (439 University Ave Suite 1920, Toronto, Ontario M5G 1Y8, Canada). Each image was calibrated and then measured using ImageJ software (ImageJ 1.42q is public domain open source software (http://rsb.info.nih.gov/ij/index.html), created by Wayne Rasband at the National Institute of Health, USA). The head phenotype was defined by measuring the angulation of the olfactory bulb [19]; then all measurements were corrected to the brain area to normalize the data.

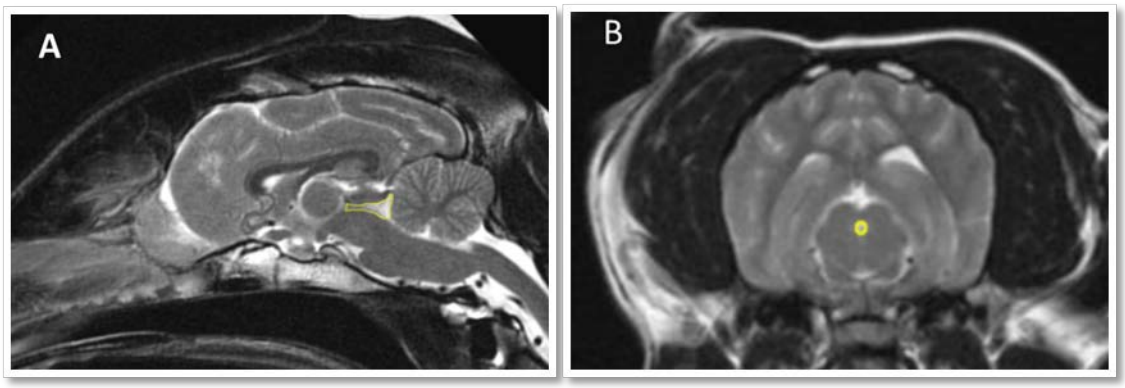

Figure 1: T2 weighted MRI of canine head defining the shape of the mesencephalic aqueduct on (A) midline sagittal plane and (B) transverse plane at the level of the colliculi.

2.2 Defining the mesencephalic aqueduct angulation

The angle between the tectum and tegmentum of the aqueduct was measured in all groups using the T2w midline sagittal slice. The angle was defined as that produced by intersecting straight lines of the ventral aspect of the tectum and the dorsal aspect of the tegmentum (Figure 2).

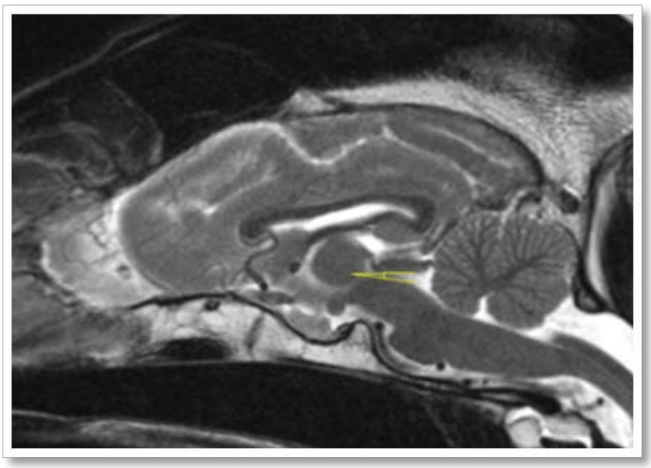

Figure 2: T2 weighted MRI midline sagittal plane representing a mesencephalic aqueductal angle measured in this study. It is defined as the angle that is produced by intersecting straight lines between the ventral aspect of the tectum and the dorsal aspect of the tegmentum.

2.3 Statistical analysis

All the data was analyzed statistically using GraphPad Prism-5 software (GraphPad Software Inc., La Jolla, USA). Descriptive statistics including the mean, standard deviation and the range were used in this study. ANOVA and t-test with post comparison tests were also used where appropriate.

3. Results

3.1 Control or Normal dogs

3.1.1 Mesencephalic aqueduct shape

The mesencephalic aqueduct was defined as the area bounded dorsally by the tectum of the mesencephalon, ventrally by the tegmentum, rostrally by the caudal commissure and caudally by the cerebellum (in the normal brain) (Figure 3).

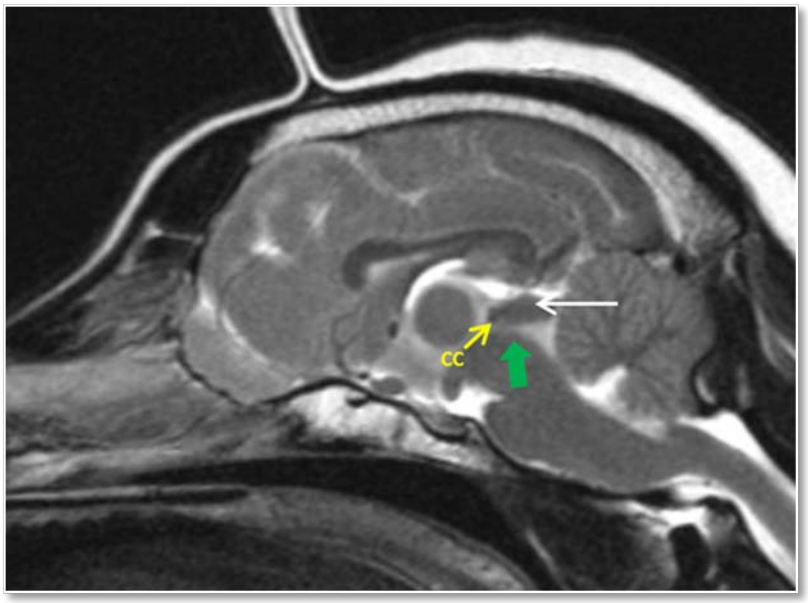

Figure 3: T2 weighted MRI midline sagittal plane showing the mesencephalic aqueduct borders. cc= caudal commissure, green arrow= tegmentum, white arrow = tectum. Note: the notch just in front of the yellow arrow.

All 32 of the control dogs had a roughly funnel to triangular shape to the mesencephalic aqueduct (Figure 1-A) with low signal intensity CSF signal rostrally at the narrowest area compared to the wider caudal part (Figure 1-A). The aqueduct had a circular shape on the transverse slice (Figure 1-B). In the most rostro-dorsal part of the aqueduct, a small notch was seen, located just after the caudal commissure (Figure 3).

3.1.2 Mesencephalic aqueduct angulation

The mesencephalic aqueduct angle was well defined in all animals of the control group. The angle ranged from 8.94 to 18.19 degrees (13.01±2.74). The angle showed no correlation with the corrected area of the

mesencephalic aqueduct. However, there was significant correlation with head phenotype (P=0.0065) only, but neither the bodyweight nor the age were significant factors (Figure 4).

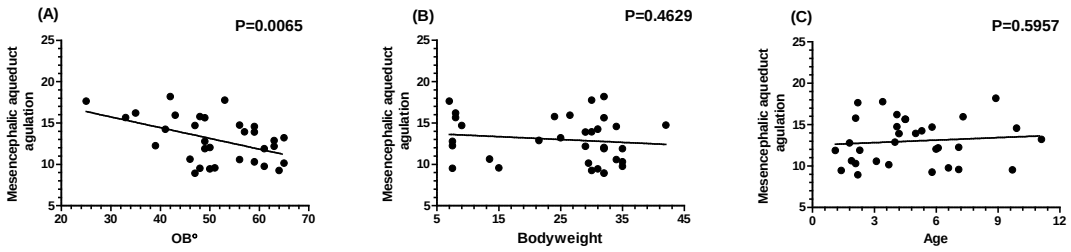

Figure 4: Linear regression graphs representing the correlation between the mesencephalic aqueduct angulation and the (A) head conformation using the olfactory bulb angulation parameter, (B) bodyweight and (C) age factors.

3.1.3 The area of the mesencephalic aqueduct and factors affecting it

The corrected area of the mesencephalic aqueduct varied between 0.43 to 0.86 cm (mean± SD = 0.64±0.11) in the control group. There was no correlation between corrected aqueduct area and head confirmation, age or bodyweight.

3.2 Abnormal Dogs (Groups 1-3)

3.2.1 The mesencephalic aqueduct

The topography of the aqueduct deviated from the defined shape in the control/normal dogs in all but G-1 where showed slightly alteration in the shape of the aqueduct (Table 1). The others revealed either compressed or enlarged aqueduct. In Group 4, all the dogs showed an apparently free open area between the aqueduct and the quadrigeminal cistern (Figure 5).

The signal intensity of the mesencephalic aqueduct altered from that seen in the controls except in G-1 where slightly changes were seen. In a hypointense signal intensity of the whole aqueduct appeared in obstructive hydrocephalus (group 2); but was hyperintense in groups (3&4) where abnormal ventriculomegaly and quadrigeminal cysts were diagnosed (Table 1 & Figure 6).

When the data for the corrected area of the mesencephalic aqueduct was compared among the groups using ANOVA, significant differences were found (P<0.0001). However, the post comparison test showed no difference between control and Group 1 (Figure 7 & Table 2).

For angulation of the mesencephalic aqueduct, significant differences (P<0.0001) were seen between groups. The post comparison test showed no significant difference between control and Group 1. The rest showed either larger or smaller angles. In obstructive hydrocephalus, smaller angles were seen 2.2±1.07. Although the largest angle was seen in Group 3 (25.54±8.08), the G 4 mean value was not dissimilar (23.16±6.32). The angle was

not calculable in 4 animals (1 in G-2 and 3 in G-3), either because of a signal void as in (Figure 8-A&B) or very irregular shape as in (Figure 8-C&D).

Table 1: Shape and signal intensity variations from normal among animals with abnormalities on mid-sagittal T2w MRI.

Groups	Shape of the aqueduct		Signal intensity of the aqueduct	
	Normal	Abnormal [enlarged, compressed or loss of the normal shape]	Normal	Abnormal [alteration in signal intensity]
Control (34)	32 (100%)		32 (100%)	
Group-1 (30)	27 (90%)	3 (10%)	20 (67%)	10 (33%)
Group-2 (3)		3 (100%)		3 (100%)
Group-3 (4)	1 (25%)	3 (75%)		4 (100%)
Group-4 (7)		7 (100%)		7 (100%)

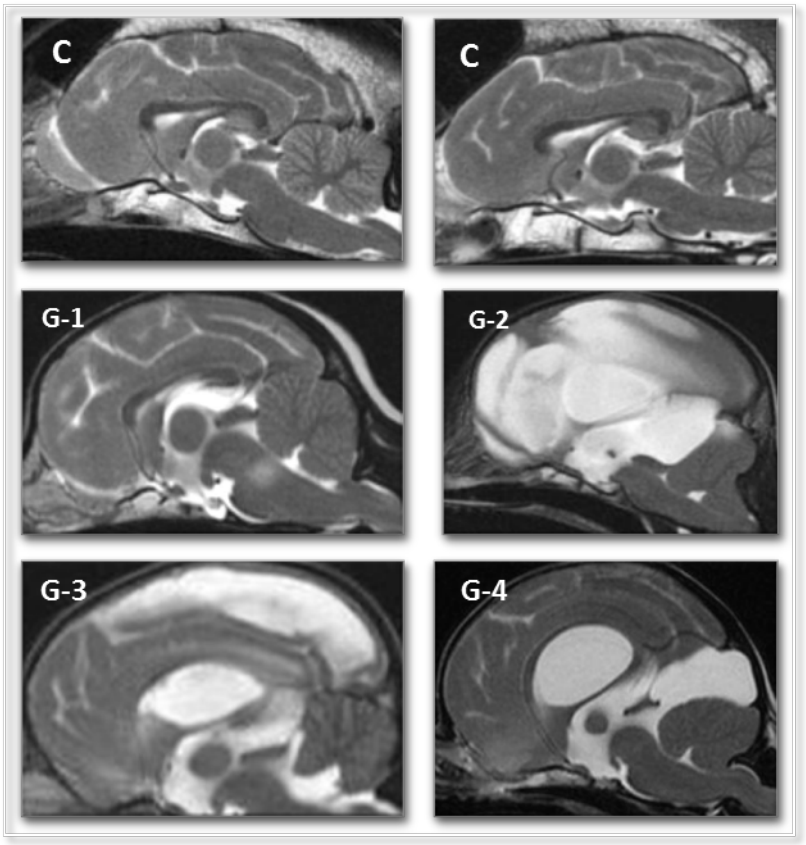

Figure 5: T2 weighted MR images representing the mesencephalic aqueduct on midline sagittal plane (C= Control group, G-1=Group-1, G-2= Group-2, G-3= Group-3 & G-4= Group-4).

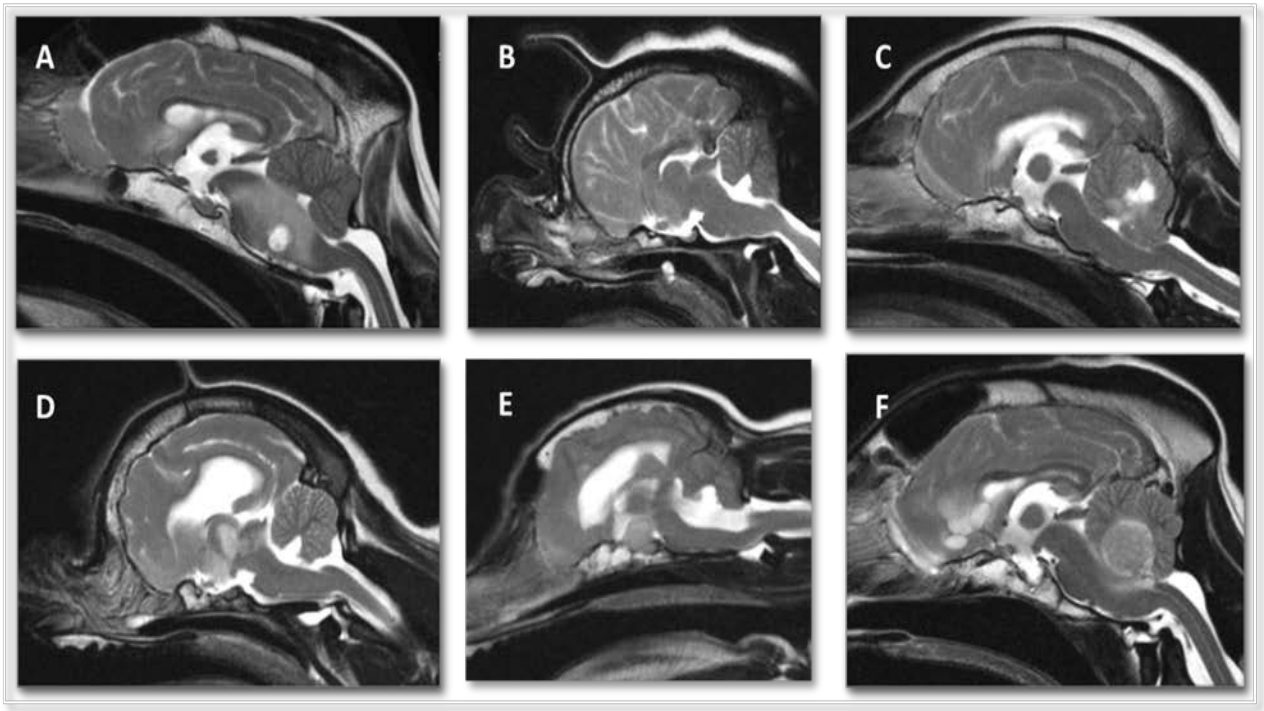

Figure 6: T2w weighted MRI midline sagittal images of group 1 representing the shape and intensity of the mesencephalic aqueduct. Note: variable changes of the mesencephalic aqueduct shape (B,D&E) and the mesencephalic aqueduct in term of intensity (A,B,C,D &E) while, the signal intensity and the shape of the mesencephalic aqueduct appears to be within normal in shape in F.

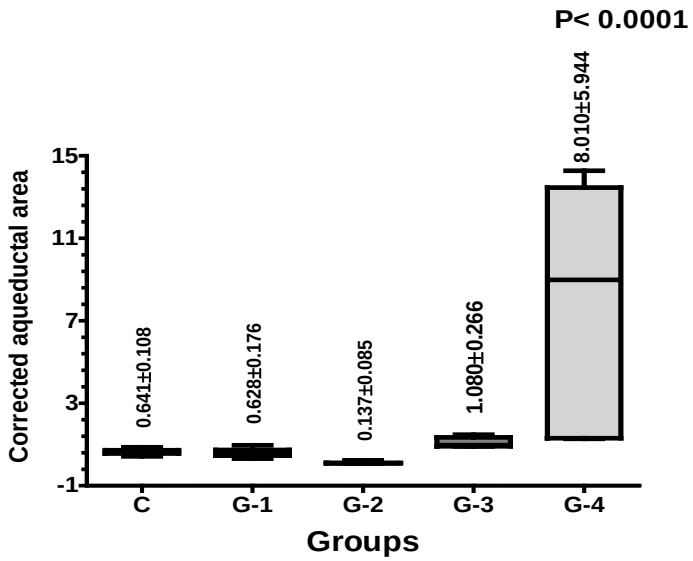

Figure 7: Box and whiskers graphs (minimum & maximum with mean and standard deviation) representing the differences among groups in term of the corrected area of the mesencephalic aqueduct which was measured on midline sagittal plane of T2 weighted MRI. [C=control, G-1=Group-1, G-2= Group-2, G-3= Group-3 & G-4=Group-4].

Table 2: The minimum, maximum, mean and the standard deviation of the values of the corrected area of the mesencephalic aqueduct were measured using T2 weighted MRI on midline sagittal plane in the following groups [C=control, G-1=group-1, G-2=group-2, G-3=group-3, G-4=group-4]. * one of the animals was excluded due to abnormalities of the mesencephalic aqueduct and its tectum where the edges was unable to be delineated.

	C	G-1	G-2	G-3	G-4
Number of values	32	30*	3	4	7
Minimum	0.4280	0.3218	0.07432	0.9058	1.280
Maximum	0.8650	0.9651	0.2327	1.477	14.28
Mean	0.6413	0.6280	0.1365	1.080	8.010
Std. Deviation	0.1082	0.1762	0.08448	0.2663	5.944

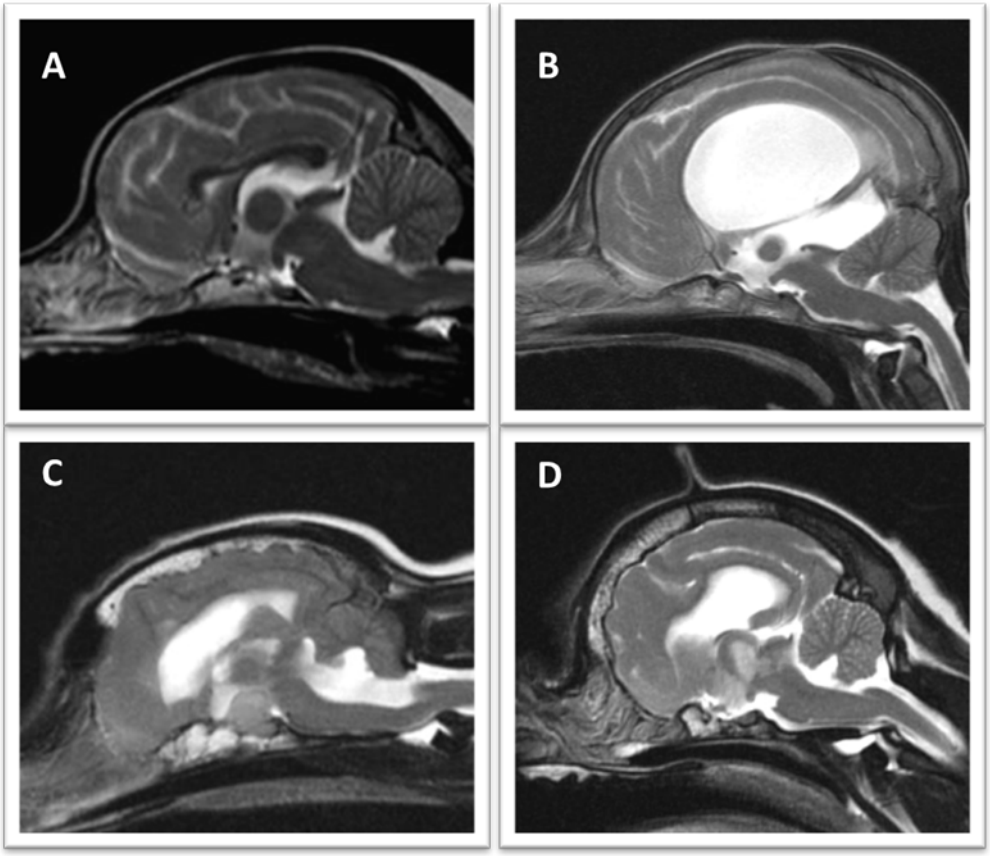

Figure 8: T2 weighted MRI midline sagittal plane showing the cases where the angulation of the mesencephalic angle was not measurable either because of apparently signal void as in (A &B) or irregular shape of the mesencephalic aqueduct and or the tectum as in (C &D).

4. Discussion

The anatomical description of the mesencephalic aqueduct was described by veterinary anatomists [3, 4] as the canal through which the CSF moves from the third to the fourth ventricle, and located within the midbrain area

[4], while, it was defined as the narrowest part of the ventricular system that connects the third to the fourth ventricle according to human anatomists [5, 6].

Descriptively, the shape of the aqueduct has been defined as having a rough funnel to triangular shape on MRI [7], equally it has described as having a gentle curve shape with concavity in its upper portion [20], caused by the retro-commissural fossa [21]. In the veterinary field, this aqueduct does not appear to have a published topographical description. In this study, the T2 weighted MRI of the canine mesencephalic aqueduct on midline sagittal plane showed that dogs too have a triangular to funnel shape. The notch, which has been identified in the man, was also seen in the dog on midline sagittal plane of T2 weighted MRI at the rostro-dorsal part of the aqueduct. The caudal part had a triangular shape but not curved as described in man (Figure 3).

On midline sagittal plane of T2w sequences the signal intensity produced by the mesencephalic aqueduct appeared to be bipartite based on the control/normal dogs, where the rostral part was hypointense relative to the caudal portion. However, this feature was altered in those dogs with detectable aqueductal abnormalities. In man, the aqueduct of sylvius produces a signal void in contrast to the rest of the ventricular system thought to be due to the increased velocity of the CSF passing through this narrow pathway [7]. It is suggested that the bipartite signal intensity seen in the dogs was due to the shape of the mesencephalic aqueduct, specifically the narrow rostral area where the CSF from the third ventricles enters. The velocity effect will ameliorate as the canal enlarges caudal, showing the more typical T2w hyperintense fluid signal compare to the rostral part. The low signal intensity becomes more void-like where a larger volume of CSF moves through a small pathway or foramen such as the aqueduct of sylvius [7]. The positioning of the aqueduct and its shape in man may lead to the signal void within the whole aqueduct comparing to the position and shape of the canine aqueduct where the relatively low signal is in the rostral but not the caudal part.

To aid recognition of aqueduct abnormality in the dog, a novel angular measurement was established between the ventral aspect of the tectum and dorsal aspect of the tegmentum. In those dogs with abnormalities, the angle appears to be different from that found in the normal brain.

The angulation of the mesencephalic aqueduct of the canine brain appears to be affected by the head conformation factor as this study showed (P=0.0065). It is suggested that the more brachycephalic the dog as defined by olfactory bulb angle, the larger the aqueduct angle. Unless significant changes within the structures surrounding the aqueduct, no significant differences in the area will be seen and this may explain why Control and Group 1 had no significant differences between them. It was found that the lumen of the mesencephalic aqueduct was not correlated to either the size of the children nor their age [11]. In our study, the above two factors also showed no correlation with the mesencephalic aqueduct corrected area.

On MRI, a complete closure in the narrowest part led to complete obstruction within the ventricular system in man [17]. Stenosis of the aqueduct has been reported as being club-shaped, broad funnel, narrow funnel, “membranous aqueduct” or atresia of the aqueduct itself using ventriculography [22]. In our cases of obstructive hydrocephalus, the stenosis led to loss of normal border shape, reduced area or and to a very low signal intensity of the mesencephalic aqueduct.

Increased aqueductal CSF flow void has been noted in MR images of people with communicating hydrocephalus [23, 24]. The signal void occurs more often in communicating normal pressure hydrocephalus than in the healthy individuals. Yet, the signal loss is less seen in acute communicating hydrocephalus or atrophy [23]. In our study the communicating hydrocephalus appeared to have less signal void (Figure 5) compared to the non-communicating hydrocephalus (obstructive hydrocephalus) as in Figure 5 & Figure 8-B.

5. Conclusions

The normal shape of the mesencephalic aqueduct can be well defined using T2w MRI on midline sagittal plane. Its area is consistent unless significant changes within the surrounding structures are seen. On MRI, the signal intensity of the mesencephalic aqueduct appeared to be altered especially when dramatic changes occur to the ventricular system. The aqueduct angle defined in this study might be developed as parameter for identifying significant aqueductal change, with the proviso that it appeared to be correlated with the degree of the brachycephalia.

References

[1] J.F. Hirsch; E. Hirsch; C. Sainte-Rose; D. Renier and A. Pierre-Khan. “Stenosis of the aqueduct of Sylvius (etiology and treatment)”. *Journal of Neurosurgical Sciences*, vol. 30, pp. 29-39, 1986.

[2] M.J. Harrison; C.M. Robert and D. Uttley. “Benign aqueduct stenosis in adults”. Journal of Neurology, Neurosurgery and Psychiatry, vol. 37, pp. 1322–1328, 1974.

[3] T. Fitzgerald. “Anatomy of the cerebral ventricles of domestic animals”. *Veterinary Medicine*, vol. 56, pp. 38-45, 1961.

[4] T. Fletcher . *Anatomy of the Dog*, Fourth Ed. Elsevier Saunders, St Louis, MO, USA, 2012.

[5] D. Woollam and J.W. Millen. “Anatomical considerations in the pathology of stenosis of the cerebral aqueduct”. Brain, vol. 76, pp. 104-112, 1953.

[6] D. McLone. “The anatomy of the ventricular system”. Neurosurgery Clinics of North America, vol. 15, pp. 33-38,2004.

[7] J.L. Sherman and C.M. Citrin. “MR imaging demonstration of CSF flow in ventriculography”. American Society of Neuroradiology, vol. 7, pp. 3-6, 1986.

[8] W.J. Hendelman. Atlas of Functional Neuroanatomy. CRC Press, Boca Raton, FL, USA, pp126-134, 2000.

[9] H.Gray. *Anatomy of the Human Body*. 23rd Ed. Lea & Febiger, Philadelphia, PA, USA, pp 517, 1936.

[10] R.S. Beckett; M.G. Netsky and H.M. Zimmerman. “Developmental stenosis of the aqueduct of sylvius”. *American Journal of Pathology*, Vol. 5, pp. 755-787, 1950.

[11] J.L. Emery and M.C.Staschak. “The size and form of the cerebral aqueduct in children”. *Brain.* vol. 95,

[12] J.González-Soriano; J.Contreras-Rodríguez; G.P. Marín; P.Martínez-Sainz and E.Rodríguez-Veiga. “Age-related changes in the ventricular system of the dog brain”. *Annals of Anatomy*, vol. 183, pp. 283-291,2001

[13] S.L. Kraft; P.R. Gavin; L.R. Wendling and V.K. Reddy. “Canine brain anatomy on magnetic resonance images”. Veterinary Radiology & Ultrasound, vol. 30, pp. 147-158. 1989.

[14] E. Leigh; E. Mackillop; I. Robertson and L. Hudson. “Clinical anatomy of the canine brain using magnetic resonance imaging”. Veterinary Radiology & Ultrasound, vol. 49, pp. 113-121, 2008.

[15] N.D. Jeffery; C.H. Thakkar and T.G. Yarrow. ”Introduction to computed tomography of the canine brain”. Journal of Small Animal Practice, vol. 33, pp. 2-10, 1992.

[16] L.C. Hudson; L. Cauzinille; J.N. Kornegay and M.B. Tompkins. “Magnetic resonance imaging of the normal feline brain”. *Veterinary Radiology & Ultrasound*, vol. 36, pp. 267-275, 1995.

[17] S.S. Kemp; R.A. Zimmerman; L.T. Bilaniuk; D.B. Hackney; H.I. Goldberg and R.I. Grossman. “Magnetic resonance imaging of the cerebral aqueduct”. Neuroradiology, vol. 29, pp. 430-436, 1987.

[18] S. Stoquart-El; P. Lehmann; C. Gondry-Jouet; A. Fichten; O. Godefroy; M.-E. Meyer and O. Baledent. “Phase-contrast MR imaging support for the diagnosis of aqueductal stenosis”. American Journal of Neuroradiology, vol. 30, pp. 209-214, 2009.

[19] A.K. Hussein.; M. Sullivan and J. Penderis. “Effect of brachycephalic, mesaticephalic, and dolichocephalic head conformations on olfactory bulb angle and orientation in dogs as determined by use of in vivo magnetic resonance imaging”. *American Journal of Veterinary Research*, vol.73, pp. 946–951, 2012.

[20] M. Schecter, “The aqueduct”. In: *Radiology of the Skull and Brain*, vol. 6. Ventricles and cisterns. T.N. Newton, O.G. Potts (eds). Mosby, St Louis, MO, USA, pp. 3363-3397. 1978.

[21] G. Stanković; V. Nikolić; L. Puškaš; B. Filipović; L. Stojšić-Džunja and D. Krivokuća. “A histological study of cerebral aqueduct”. *Medicinski Pregled*, vol. 58, pp. 534-540, 2005.

[22] M.M. Schechter; L.H. Zingesser. “The radiology of aqueductal stenosis”. *Radiology*, vol. 88, pp. 905-916, 1967.

[23] W.G. Bradley; K.E. Kortman and B. Burgoyne. “Flowing cerebrospinal fluid in normal and hydrocephalic states: appearance on MR images”. *Radiology*, vol. 159, pp. 611–616, 1986.

[24] C. Jack; B. Mokri; E. Laws; O.W. Houser, H. Baker and R.C. Petersen. “MR findings in normal-pressure hydrocephalus: significance and comparison with other forms of dementia”. *Journal of Computer Assisted Tomography*, vol. 11, pp. 923–931, 1987.